ACS APPLIED MATERIALS & INTERFACES

Research Article

www.acsami.org

Antimicrobial Hyaluronic Acid/Poly(amidoamine) Dendrimer Multilayer on Poly(3-hydroxybutyrate-*co*-4-hydroxybutyrate) Prepared by a Layer-by-Layer Self-Assembly Method

Jiezhao Zhan,[†] Lin Wang,[†] Sa Liu, Junjian Chen, Li Ren,* and Yingjun Wang*

School of Materials Science and Engineering, South China University of Technology, Guangzhou 510641, China

National Engineering Research Center for Tissue Restoration and Reconstruction, Guangzhou 510006, China

Guangdong Province Key Laboratory of Biomedical Engineering, South China University of Technology, Guangzhou 510006, China

Supporting Information

ABSTRACT: In this article, we prepared hyaluronic acid/poly(amidoamine) dendrimer (HA/PAMAM) multilayers on a poly(3-hydroxybutyrate-*co*-4-hydroxybutyrate) [P(3HB-4HB)] substrate by a layer-by-layer self-assembly method for antimicrobial biomaterials. The results of ζ potential and quartz crystal microbalance with dissipation (QCM-D) showed that HA/PAMAM multilayers could be formed on the substrate layer by layer. We used QCM-D to show that both the HA outer layer and the PAMAM outer layer exhibited good protein-resistant activity to bovine serum albumin and bacterial antiadhesion activity to *Escherichia coli*. By a live/dead assay and the colony counting method, we found that the PAMAM outer layer could also exhibit bactericidal activity against *E. coli*, while the HA outer layer had no bactericidal activity. Both the bacterial antiadhesion activity and the bactericidal activity of the samples could be maintained even after storage in phosphate-buffered saline for up to 14 days. An in vitro MTT assay showed that the multilayers had no cytotoxicity to L929 cells, and HA molecules in the multilayers could improve the biocompatibility of the film.

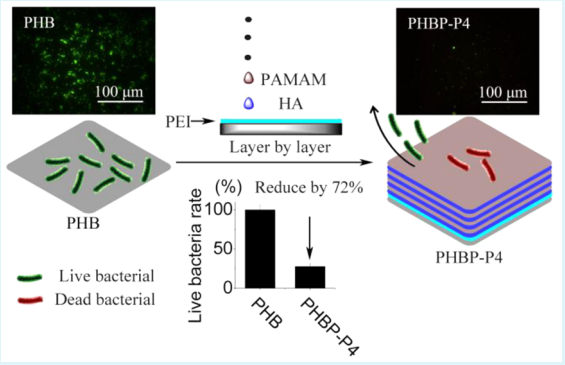

KEYWORDS: *antimicrobial activity, PAMAM dendrimer, hyaluronic acid, layer by layer, QCM-D*

1. INTRODUCTION

Bacterial infection is a serious problem in the field of biomaterial because it could lead to the destruction of local tissues, patient disability and morbidity, and even death.[1] Preparing antimicrobial films on biomaterials that have bacterial antiadhesion activity or bactericidal activity is a suitable way to resolve biomaterial-associated infection.[2−7] For example, preparing a silk sericin film with bacterial antiadhesion activity on the substrate could reduce the adhesion of *Staphylococcus aureus* and *Staphylococcus epidermidis* evidently, which would inhibit the formation of a biofilm on the implant.[5] Meanwhile, preparing a bactericidal film with an antimicrobial agent, such as antibiotic or antimicrobial peptide, on a substrate in order to kill the bacteria in contact with the biomaterial could also inhibit bacterial infection.[2,6,7] However, there are still many problems with these antimicrobial films. The film with bacterial antiadhesion activity did not successfully kill the bacteria in contact with it.[5] For bactericidal films, bacterial resistance as well as cytotoxicity and side effects are significant problems.[6,7] Therefore, the question of how to resolve these problems to prepare antimicrobial films on biomaterials is of great interest.

In this paper, we use poly(3-hydroxybutyrate-*co*-4-hydroxybutyrate) [P(3HB-4HB)] as the substrate to prepare a film with both bacterial antiadhesion activity and bactericidal activity. We chose P(3HB-4HB) as our substrate because it was suitable as an implant for tissue engineering because of its excellent biodegradability and biocompatibility and adjustable mechanical properties.[8−10] We chose poly(amidoamine) dendrimers (PAMAM) as the bactericidal agent in our system because the amino groups around PAMAM could target and disrupt the bacterial membrane.[11,12] This membrane-targeting bactericidal agent is less likely to result in bacterial resistance compared to protein-targeting antimicrobial agents, such as antibiotics. In addition, as reported, PAMAM was more effective on Gram-negative bacteria,[13] whose double-cell and powerful membrane pumps make them more difficult to kill than Gram-positive bacteria.[14] Meanwhile, in our system, we chose hyaluronic acid (HA) as the bacterial antiadhesion agent because it showed negative charge, similar to a bacterial membrane, and it could inhibit bacterial adhesion onto the substrate.[15,16] Moreover, as one component of the extracellular matrix, HA exists in advanced living organisms and has good biocompatibility,[17] which should decrease the cytotoxicity of bactericidal PAMAM molecules.[13]

Received: March 14, 2015
Accepted: June 10, 2015
Published: June 10, 2015

DOI: 10.1021/acsami.5b02262
ACS Appl. Mater. Interfaces 2015, 7, 13876−13881

Because PAMAM and HA showed opposite charge, we use the layer-by-layer (LBL) self-assembly method to prepare the multilayers of HA and PAMAM on P(3HB-4HB). LBL is a promising approach to fabricate functional surfaces with well-defined architectures.[18] It offers a wide choice of available molecules, flexibility and simplicity of construction, structural precision, and the ability to coat materials with any shape and dimension. With this method, the multilayer can be prepared on the surfaces through consecutive deposition of polyanions and polycations via electrostatic interactions. Neoh et al. constructed the HA/chitosan polyelectrolyte multilayers on a titanium surface and showed that the multilayers could inhibit bacterial adhesion.[15] Hammond et al. used a LBL method to construct multilayers containing PAMAM on a micelle system to release drugs, which presented an excellent antimicrobial property against *Staphylococcus aureus*.[19]

In the present study, we use quartz crystal microbalance with dissipation (QCM-D) and ζ potential to characterize formation of the multilayer and use QCM-D to characterize the protein-resistant activity of the multilayer. We also use QCM-D, live/dead assay, and the colony counting method to characterize the antimicrobial activity of the substrate against Gram-negative bacteria *Escherichia coli*, and we use L929 cells to test the biocompatibility of the multilayers.

2. MATERIALS AND METHODS

2.1. Materials. Hyaluronic acid (HA; M_w = 1.0−1.5 × 10^6 Da) was purchased from Guangzhou QiYun Biological Technology Co., Ltd. G5 poly(amidoamine) dendrimer (PAMAM; M_w = 20000 Da) was purchased from Sigma-Aldrich. Polyethylenimine (PEI; M_w = 1 × 10^4 Da) was obtained from Shanghai YuanYe Biological Technology Co., Ltd., and ethylene dichloride (EDC)/*N*-hydroxysuccinimide (NHS) was purchased from Sigma. Bovine serum albumin (BSA) was obtained from Guangzhou JiYun Biological Technology Co., Ltd., and poly(3-hydroxybutyrate-*co*-4-hydroxybutyrate) [P(3HB-4HB)] was obtained from Shenzhen Ecomann Biological Technology Co., Ltd. A live/dead BacLight Bacterial Viability Kit L7012 was obtained from Molecular Probes, Inc. All of the antibacterial test- and cell-assay-related agents were purchased from Sigma.

2.2. Sample Preparation. *2.2.1. Preparation of the P(3HB-4HB) Substrate.* We first prepared P(3HB-4HB) films (the structure is shown in Figure S1a in the Supporting Information, SI) on silicon wafers (1 cm × 1 cm × 0.1 cm) or quartz crystals (QSX301, Q-Sense, Sweden) by spin-coating with 0.5% (w/v) solutions of P(3HB-4HB) (chloroform:tetrahydrofuran = 9:1 in volume). The sample, which was placed in an oven for 2 h at 60 °C, was abbreviated as PHB.

2.2.2. Preparation of the PAMAM Layer on PHB. PHB was treated with oxygen plasma in the DL-01 model plasma generator (Suzhou Omega Machinery Electronic Technology Co. Ltd., China) at 50 W for 5 min. Then, it was immersed in a 80 μg/mL PAMAM solution (the structure is shown in Figure S1b in the SI) in PBS for 1 h, rinsed with PBS buffer three times, dried with nitrogen flow, and abbreviated as PHB−PAMAM.

2.2.3. Preparation of the HA/PAMAM Multilayer on PHB by a LBL Process. HA (the structure is shown in Figure S1c in the SI) and PAMAM were diluted in PBS buffer at a concentration of 80 μg/mL. Before the LBL process, a PEI layer was first deposited by immersing the PHB in a PEI solution (1 mg/mL in PBS) for 1 h. After it was washed with Milli-Q water, the sample was dried with a nitrogen flow and abbreviated as PHBP. Then, PHBP was immersed in a HA solution for 15 min and rinsed with PBS buffer three times. After that, the sample was immersed in a PAMAM solution for 15 min and rinsed with PBS buffer three times. The deposition cycle was repeated until the indicated sample (PHBP-Hn or PHBP-Pn) was completed. All of the sample abbreviations are shown in Table S1 in the SI.

2.3. Characterization of the LBL Process. *2.3.1. Characterization of the LBL Process with the ζ Potential Assay.* The ζ potential of the sample was obtained using an electrokinetic analyzer (Anton Paar SurPASS, Graz, Austria). For determination of ζ, streaming current measurements were performed using an adjustable gap cell (Anton Paar SurPASS, Graz, Austria). A potassium chloride (KCl) solution (1.0 mM) was used as the background electrolyte, and 0.1 M potassium hydroxide and 0.1 M hydrochloric acid solutions were used to adjust the pH value to 7.2. The ζ potential is calculated according to the formula

$$\zeta = \frac{\mathrm{d}I}{\mathrm{d}P}\,\frac{\eta}{\varepsilon\varepsilon_0}\,\frac{L}{A}$$

where $\mathrm{d}I/\mathrm{d}P$ represents the slope of the streaming current versus differential pressure, η is the electrolyte viscosity, ε represents the dielectric coefficient of the electrolyte, ε_0 is the permittivity, and L/A is the ratio of length L and cross section A of the streaming channel.

2.3.2. Characterization of the LBL Process with QCM-D Assay. PHBP on the gold-coated silicon QCM electrodes were put into the sensor chambers of the Q-Sense E4 QCM-D system, and the LBL process was monitored as follows. Briefly, at first, a HA solution was introduced to the substrate for 15 min and rinsed with PBS buffer until the frequency was balanced. After that, a PAMAM solution was introduced to the substrate for 15 min and rinsed with PBS buffer until the frequency was balanced. The deposition cycle above was repeated until the indicated sample was completed.

2.4. BSA Adsorption. BSA adsorption of the surfaces was measured by QCM-D. Briefly, first, the BSA solution (dissolved in PBS buffer at a concentration of 50 μg/mL) was introduced to the samples. After balancing, PBS buffer was introduced again to wash off the nonadsorbed protein. The ΔF (the frequency change of the resonator) curve of the sample was used to illustrate the BSA adsorption mass.

2.5. Antimicrobial Assay. *2.5.1. Bacterial Culture. E. coli* was used to test the antimicrobial activity of the samples. A single colony of *E. coli* was inoculated in 5 mL of Luria-Bertani (LB) medium overnight at 37 °C. Then, 1 mL of the *E. coli* suspension was inoculated in 50 mL of a fresh LB medium and incubated for 5 h with shaking (250 rpm) at 37 °C to achieve mid-log-phase growth.

2.5.2. QCM-D Assay of the Bacterial Antiadhesion Activity. To evaluate the bacterial antiadhesion activity of the samples (PHB, PHB-PAMAM, PHBP-H4, and PHBP-P4) with QCM-D, different solutions were injected sequentially into the QCM-D system in the following order: (i) a PBS background solution for 10 min; (ii) suspended bacteria in PBS at a concentration of 10^8 cfu/mL for 3 h; (iii) a PBS solution without bacteria for 1 h. The ΔF curve was used to illustrate the bacterial antiadhesion activity of each sample.

2.5.3. Colony Counting Assay of the Antimicrobial Activity. Prior to bacterial seeding, the samples (1 cm × 1 cm) were sterilized by 70% isopropyl alcohol for 0.5 h, placed in a 24-well culture plate, and washed three times with PBS buffer. The *E. coli* suspension was adjusted to a concentration of 1 × 10^8 cfu/mL in PBS. Then, 750 μL of the bacterial suspension was added into each well to fully cover the surface of the samples. The bacteria were cultured with shaking at 37 °C (150 rpm). After incubation for 3 h, the samples were taken out, washed gently with PBS buffer and immersed in 2 mL of sterile PBS buffer. This system was treated with an ultrasonic bath for 10 min to detach the bacteria. Then, the detached bacteria were evaluated by a serial dilution method with agar plates.

To evaluate the stability of the antimicrobial activity of the films, after degradation in PBS for 14 days, the samples were treated with *E. coli* as above.

2.6. Biocompatibility of the Samples. L929 cells were used to study the biocompatibility of the samples. The cells were cultured in a 1640 medium (PAA Laboratories GmbH, Austria) containing 10% fetal bovine serum (FBS) and in an incubator at 37 °C and a 5% CO_2 atmosphere. The medium was replaced every third day.

All samples (1 cm × 1 cm) used for cell tests were sterilized with 70% isopropyl alcohol for 2 h. After sterilization, the samples were placed individually into the 24-well plates, and the L929 cells were added directly onto each sample (5000 cells in 1 mL of 1640 media

DOI: 10.1021/acsami.5b02262
ACS Appl. Mater. Interfaces 2015, 7, 13876−13881

containing 10% FBS per sample). They were cultured for 3 days, and the culture medium was replaced every 2 days.

After the materials were cultured for 3 days, the biocompatibility of the materials was evaluated with 3-(4,5-dimethylthiazol-2-yl)-2,5-diphenyltetrazolium bromide [MTT, Sigma] assay. Briefly, at an indicated time point, the samples were transferred to a new 24-well plate and washed three times with PBS. Then, 750 μL of a complete medium with 75 μL of MTT (5 mg/mL in PBS) was added to each disk. After incubation for 4 h at 37 °C in the dark, the MTT solution was removed, and the formazan crystals were dissolved in 400 μL of dimethyl sulfoxide for 20 min. The optical density value of the dissolved solute was measured with an ELISA plate reader (Varioskan Flash 3001, Thermo, Finland) at 570 nm.

3. RESULTS AND DISCUSSION

3.1. LBL Process Assay. The LBL process scheme and ζ potential of the indicated samples are shown in Figure 1. We

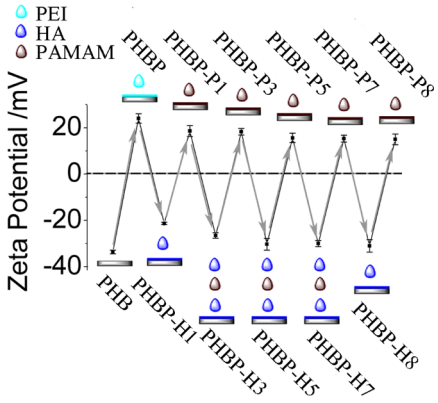

Figure 1. LBL process schemes and ζ potential of the indicated samples. The drops mean that the sample was treated with the referenced liquid solutions, and the number of drops means the number of layers formed on the substrate.

see that during the LBL process the ζ potential changed accordingly. At first, the ζ potential of PHB was -33.6 ± 0.8 mV, and the ζ potential of PHBP changed to 24.0 ± 2.0 mV after formation of the PEI film. Meanwhile, the X-ray photoelectron spectroscopy (XPS) N 1s high-resolution spectra (Figure S2 in the SI) show that, compared to PHB, both PHBP and PHB-PAMAM exhibited evident N 1s peaks at 400 eV, which also demonstrated that PAMAM or PEI was deposited on the surface of PHB successfully. After that, the trend of the ζ potential alternated between negative and positive with the formation of HA and PAMAM films, which demonstrated that the LBL process was successful. The HA outer layer showed negative charge and the PAMAM outer layer positive charge under neutral conditions.[20−22]

QCM-D was also used to characterize the LBL process, and the results are shown in Figure 2. We see that at the beginning, after a HA solution was introduced to PHBP, ΔF decreased during the first 3 min. Then, the decline rate reduced, and ΔF reached −20.1 Hz after 10 min. This indicated that there was an increase of mass,[23] which was caused by the deposition of HA molecules onto the substrate. Meanwhile, there was no change of ΔF after PBS addition, which indicated that the interaction between the HA molecules and PHBP was strong and the HA layer was stable. When a PAMAM solution was introduced, the trend was similar to that of a HA solution and ΔF reached −76.8 Hz. However, after reaching a balance, ΔF increased slightly when PBS was added, which indicated that

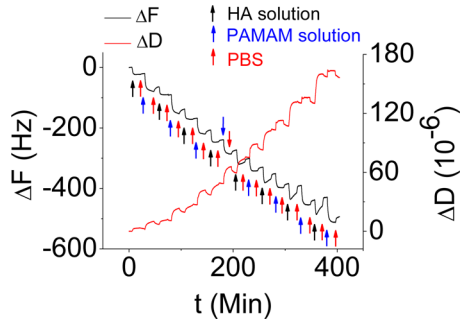

Figure 2. Frequency change (ΔF) and dissipation change (ΔD) of the resonator during the LBL process with QCM-D assay. Data were collected from the third overtone.

part of PAMAM bonded weakly to the substrate and was washed off by PBS. During the LBL process, ΔF (the frequency change of resonator) changed in value, which illustrated that the HA/PAMAM multilayer was prepared layer by layer successfully.

We used $\Delta F-\Delta D$ plots from the QCM-D results to illustrate the structure of the multilayers on the surface (ΔD is the dissipation factor change of the resonator), and the results are shown in Figure 3. As reported, a larger slope of the plots

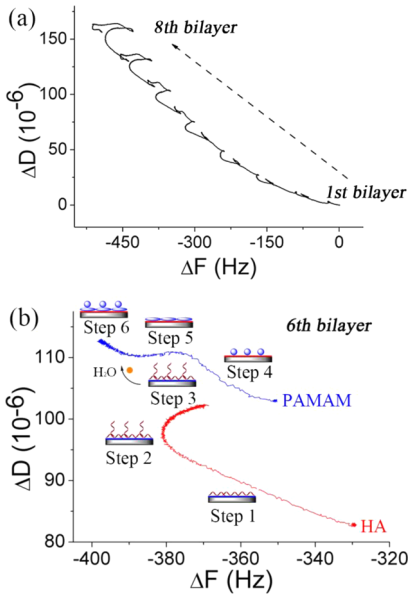

Figure 3. $\Delta F-\Delta D$ plots during the LBL process with QCM-D assay: (a) whole LBL process forming the first and eighth bilayers; (b) sixth bilayer process. Data were collected from the third overtone.

means that the films had a looser structure.[24] Figure 3a shows that the slopes of the plots changed during multilayer formation, which indicates that the structure of each layer was different. For example, Figure 3b shows the $\Delta F-\Delta D$ plots of the sixth bilayer. We see that, during the addition of a HA solution, the slope of the plots could be divided into three steps (steps 1−3 in Figure 3b). At first, HA was adsorbed quickly onto the surface (step 1). Second, the chains of HA were rearranged to adsorb more HA, which tended to make the film looser (step 2). Third, as in step 3, the increase in ΔF and ΔD indicates that the mass of the film decreased and the construction of the film became even looser. This might be caused by cross-linking between HA and PAMAM, which

DOI: 10.1021/acsami.5b02262
ACS Appl. Mater. Interfaces 2015, 7, 13876−13881

causes extrusion of the water molecules. These water molecules lead to a decrease in mass and some holes in the film, which caused the film to become looser. Formation of the PAMAM layer could also be divided into three steps (steps 4−6 in Figure 3b). However, it was different from that of the HA layer. At first, the PAMAM molecules were adsorbed quickly onto the surface (step 4), which was similar to HA. After that, the decrease in ΔF and the balance of ΔD in step 5 indicate that more PAMAM molecules were adsorbed on the surface and the PAMAM layer became denser. Thus, the globular PAMAM structure became elliptical. Finally, the decrease in ΔF and the increase in ΔD in step 6 indicate that more globular PAMAM molecules were adsorbed onto the surface. At this step, these PAMAM molecules could maintain their structure because of intermolecular repulsion.

3.2. BSA Adsorption Assay. The results above show that the HA/PAMAM multilayer can be prepared on the PHBP substrate layer by layer. We then chose PHBP-H4 as the HA outer sample and PHBP-P4 as the PAMAM outer sample for the next experiments. The interaction between the protein and surface of the material will impact the bacterial response on the material. Protein adsorption will promote adhesion and growth of bacteria on the surface of the material.[25] Thus, a resistance protein adsorption surface is beneficial to improve the antibacterial property of the material. Then, we used QCM-D to characterize the antiabsorption activity of the indicated samples to BSA, and the results are shown in Figure 4. After

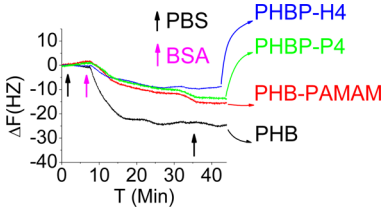

Figure 4. QCM-D assay for BSA adsorption on the indicated samples. Black arrows indicate the times of PBS additions, and purple arrows indicate the times of BSA solution rinses.

introduction of the BSA solution, the frequency of PHB was −25.2 Hz when the BSA adsorption was balanced, and the values of PHB-PAMAM, PHBP-H4, and PHBP-P4 were −15.6, −9.1, and −13.5 Hz, respectively. This indicates that all of the samples with films presented anti-BSA adsorption. The adsorption mass of BSA calculated from Figure 4 with *Q-Tools* (data processing software of QCM-D) is shown in Table S2 in the SI. This shows that the mass of BSA on PHB was 446 ng/cm^2. Compared to that on PHB, the masses of BSA on PHB-PAMAM, PHBP-H4, and PHBP-P4 were reduced by 38.1%, 64.1%, and 46.6% and had values of 276, 160, and 238 ng/cm^2, respectively. The anti-BSA adsorption trend was PHBP-H4 > PHBP-P4 > PHB-PAMAM, which is similar to the hydrophilicity trend of the samples shown in Figure S3 in the SI. Because the hydrophobic surface was prone to protein adsorption,[26] the hydrophilic HA in the multilayers could inhibit BSA adsorption.[27,28]

3.3. Antimicrobial Activity Assay. The construction of a bacterial antiadhesion surface is a suitable way to resolve biomaterial-associated infection. In order to know whether the films we prepared have the activity of bacterial antiadhesion, we also used QCM-D to monitor the real-time interaction between bacteria and surfaces. The results shown in Figure 5

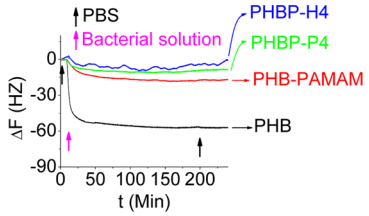

Figure 5. QCM-D assay for bacterial adhesion on the indicated samples. Black arrows indicate the times of PBS additions, and purple arrows indicate the times of bacterial solution rinses.

demonstrate that, compared to the PHB, all of the surfaces with multilayers presented antiadhesion activity to *E. coli*. After infusion of a bacterial solution for 3 h, the frequency of PHB was −56.7 Hz, while those of PHB-PAMAM, PHBP-P4, and PHBP-H4 were −18.1, −10.7, and −8.2 Hz, respectively. There was no change of the frequency after infusion with PBS. Using the results in Figure 5 with *Q-Tools*, the mass values of *E. coli* on PHB, PHB-PAMAM, PHBP-P4, and PHBP-H4 are shown in Table S3 in the SI. Because HA has a negative charge, which was the same as that of *E. coli*, it has the activity to inhibit adhesion of bacteria.[15,29] Accordingly, PHBP-H4 showed the best antiadhesion behavior, and the bacteria amount reduced by 85.4% compared to that of PHB. Interestingly, although PAMAM molecules showed a charge opposite to that of *E. coli*, both PHBP-P4 and PHB-PAMAM showed bacterial antiadhesion behavior. The masses of bacteria were about 19.0% and 32.0% of that on PHB. This may be because PAMAM had bactericidal properties toward *E. coli*, which led to a loss of cellular content. Furthermore, the bacterial antiadhesion behavior of PHBP-P4 was a little better than that of PHB−PAMAM, which indicated that the PAMAM molecules on the outer layer were affected by the HA molecules under the outer layer. In addition, the antiadhesion trend of the samples was also PHBP-H4 > PHBP-P4 > PHB-PAMAM, which was similar to the anti-BSA adsorption and hydrophilicity trends of the samples.

The bactericidal activity of the surface is also a suitable way to resolve biomaterial-associated infection. Live/dead assay was used as a viability indicator to characterize the antimicrobial activity (containing bacterial antiadhesion activity and bactericidal activity) of the samples, and the results are shown in Figure S4 in the SI. They show that PHB-PAMAM, PHBP-H4, and PHBP-P4 presented bacterial antiadhesion activity against *E. coli* compared to PHB after 3 h and have a trend similar to that shown by the QCM-D results in Figure 5. Besides bacterial antiadsorption activity, the PHB-PAMAM and PHBP-P4 that we prepared also had bactericidal activity. As shown in Figure S4 in the SI, most of the bacteria on PHB-PAMAM and PHBP-P4 were killed (which showed red fluorescence). However, the bacteria on PHBP-H4 were alive (which showed green fluorescence).

In order to characterize the antimicrobial activity of the samples quantitatively, the colony counting method was used, and the results are shown in Figure 6a. Compared to PHB, PHB-PAMAM, PHBP-H4, and PHBP-P4 showed evident antimicrobial activity. The live bacterial amounts on these surfaces were approximately 33.9%, 36.4%, and 27.8%, respectively, compared to that on PHB. Figure 6b shows that, after degradation for 14 days, PHB-PAMAM, PHBP-H4, and PHBP-P4 could also show good antimicrobial activity, and the live bacterial amounts on these surfaces were approximately

DOI: 10.1021/acsami.5b02262
ACS Appl. Mater. Interfaces 2015, 7, 13876−13881

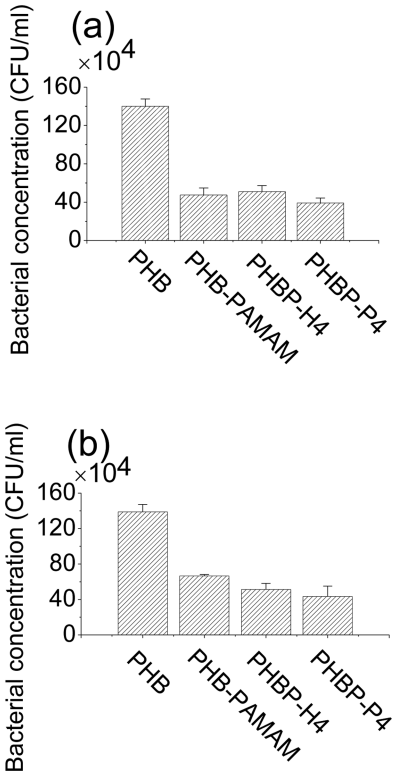

Figure 6. Antimicrobial activity of the indicated samples against *E. coli* after 3 h of incubation before (a) and after (b) degradation in PBS for 14 days (n = 3).

47.3%, 36.9%, and 31.2%, respectively, compared to that on PHB. This demonstrates that the multilayers on the substrate had good stability.

3.4. Biocompatibility Assay. The biocompatibility of the samples was characterized with MTT assay, and the results are shown in Figure 7. Although other papers reported that

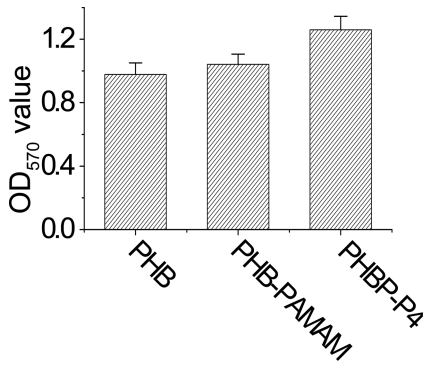

Figure 7. Biocompatibility of the indicated samples to L929 cells in 3 days by MTT assay (n = 3).

PAMAM was toxic, PHB-PAMAM showed biocompatibility similar to that of PHB. This may be caused by the low loading amount of PAMAM on the surface.[30] Meanwhile, as the HA molecule has a specific role in improving the adhesion of cells,[31,32] the PHBP-P4 has the best biocompatibility. The number of cells on PHBP-P4 was approximately 1.27 times that on PHB. The results illustrated that the surfaces that we prepared had good biocompatibility as biomaterials.

4. CONCLUSION

In this paper, a HA/PAMAM multilayer was prepared on the P(3HB-4HB) substrate by a LBL self-assembly method. After modification, all of the samples showed good antimicrobial activity and biocompatibility. Among the samples, PHBP-H4 only presented bacterial antiadhesion activity, while PHBP-P4 presented both bacterial antiadhesion activity and bactericidal activity. Meanwhile, the antimicrobial activity of these films could last up to 14 days. The HA molecules in PHBP-P4 also improved the biocompatibility of the film. Above all, the samples that we prepared with HA and PAMAM by a LBL process show considerable potential as antibacterial biomaterials.

■ ASSOCIATED CONTENT

Ⓢ Supporting Information

QCM-D formula to calculate the mass of the adsorbed layer, chemical structures of P(3HB-4HB), PAMAM, and HA, and detailed experimental methods as well as the results of XPS and the water contact angle and live/dead assays, abbreviations of the samples, and amounts of BSA and bacterial adsorption. The Supporting Information is available free of charge on the ACS Publications website at DOI: 10.1021/acsami.5b02262.

■ AUTHOR INFORMATION

Corresponding Authors

*E-mail: psliren@scut.edu.cn.
*E-mail: imwangyj@scut.edu.cn.

Author Contributions

The manuscript was written through contributions of all authors. All authors have given approval to the final version of the manuscript. These authors contributed equally.

Author Contributions

†These authors contributed equally.

Notes

The authors declare no competing financial interest.

■ ACKNOWLEDGMENTS

The authors are thankful for the National Key Technologies R&D Program (Grant 2012BAI17B02), National Nature Science Foundation of China (Grants 51232002, 51273072, and 51302088), Nature Science Foundation of Guangdong (Grants 2012A080203010 and 2012A080800015), and the Fundamental Research Funds for the Central Universities (Grant D215138W).

■ REFERENCES

(1) Darouiche, R. O. Treatment of Infections Associated with Surgical Implants. *N. Engl. J. Med.* **2004**, *350*, 1422−1429.
(2) Tiller, J. C.; Liao, C.-J.; Lewis, K.; Klibanov, A. M. Designing Surfaces That Kill Bacteria on Contact. *Proc. Natl. Acad. Sci. U. S. A* **2001**, *98*, 5981−5985.
(3) Bílek, F.; Sulovská, K.; Lehocký, M.; Sáha, P.; Humpolíček, P.; Mozetič, M.; Junkar, I. Preparation of Active Antibacterial Ldpe Surface through Multistep Physicochemical Approach II: Graft Type Effect on Antibacterial Properties. *Colloids Surf., B* **2013**, *102*, 842−848.
(4) Wiarachai, O.; Thongchul, N.; Kiatkamjornwong, S.; Hoven, V. P. Surface-Quaternized Chitosan Particles as an Alternative and Effective Organic Antibacterial Material. *Colloids Surf., B* **2012**, *92*, 121−129.
(5) Zhang, F.; Zhang, Z.; Zhu, X.; Kang, E.-T.; Neoh, K.-G. Silk-Functionalized Titanium Surfaces for Enhancing Osteoblast Functions and Reducing Bacterial Adhesion. *Biomaterials* **2008**, *29*, 4751−4759.

DOI: 10.1021/acsami.5b02262
ACS Appl. Mater. Interfaces 2015, 7, 13876−13881

(6) Wang, L.; Chen, J.; Cai, C.; Shi, L.; Liu, S.; Ren, L.; Wang, Y. Multi-Biofunctionalization of a Titanium Surface with a Mixture of Peptides to Achieve Excellent Antimicrobial Activity and Biocompatibility. *J. Mater. Chem. B* **2015**, *3*, 30−33.
(7) Wang, L.; Chen, J.; Shi, L.; Shi, Z.; Ren, L.; Wang, Y. The Promotion of Antimicrobial Activity on Silicon Substrates Using a "Click" Immobilized Short Peptide. *Chem. Commun.* **2014**, *50*, 975−977.
(8) Chen, G.-Q. A Microbial Polyhydroxyalkanoates (Pha) Based Bio- and Materials Industry. *Chem. Soc. Rev.* **2009**, *38*, 2434−2446.
(9) Chen, G.-Q.; Wu, Q. The Application of Polyhydroxyalkanoates as Tissue Engineering Materials. *Biomaterials* **2005**, *26*, 6565−6578.
(10) Zhan, J.; Tian, X.; Zhu, Y.; Wang, L.; Ren, L. Oxygen Plasma Modified P (3hb-4hb) Used as Anticoagulant Materials. *Appl. Surf. Sci.* **2013**, *280*, 564−571.
(11) Wang, L.; Erasquin, U. J.; Zhao, M.; Ren, L.; Zhang, M. Y.; Cheng, G. J.; Wang, Y.; Cai, C. Stability, Antimicrobial Activity, and Cytotoxicity of Poly(Amidoamine) Dendrimers on Titanium Substrates. *ACS Appl. Mater. Interfaces* **2011**, *3*, 2885−2894.
(12) Lopez, A. I.; Reins, R. Y.; McDermott, A. M.; Trautner, B. W.; Cai, C. Antibacterial Activity and Cytotoxicity of Pegylated Poly-(Amidoamine) Dendrimers. *Mol. BioSyst.* **2009**, *5*, 1148−1156.
(13) Wang, L.; Erasquin, U. J.; Zhao, M.; Ren, L.; Zhang, M. Y.; Cheng, G. J.; Wang, Y.; Cai, C. Stability, Antimicrobial Activity, and Cytotoxicity of Poly(Amidoamine) Dendrimers on Titanium Substrates. *ACS Appl. Mater. Interfaces* **2011**, *3*, 2885−2894.
(14) Higgins, M. K.; Bokma, E.; Koronakis, E.; Hughes, C.; Koronakis, V. Structure of the Periplasmic Component of a Bacterial. *Drug Efflux Pump* **2004**, *101*, 9994−9999.
(15) Chua, P.-H.; Neoh, K.-G.; Kang, E.-T.; Wang, W. Surface Functionalization of Titanium with Hyaluronic Acid/Chitosan Polyelectrolyte Multilayers and Rgd for Promoting Osteoblast Functions and Inhibiting Bacterial Adhesion. *Biomaterials* **2008**, *29*, 1412−1421.
(16) Hu, X.; Neoh, K.-G.; Shi, Z.; Kang, E.-T.; Poh, C.; Wang, W. An in Vitro Assessment of Titanium Functionalized with Polysaccharides Conjugated with Vascular Endothelial Growth Factor for Enhanced Osseointegration and Inhibition of Bacterial Adhesion. *Biomaterials* **2010**, *31*, 8854−8863.
(17) Mason, M.; Vercruysse, K. P.; Kirker, K. R.; Frisch, R.; Marecak, D. M.; Prestwich, C. D.; Pitt, W. G. Attachment of Hyaluronic Acid to Polypropylene, Polystyrene, and Polytetrafluoroethylene. *Biomaterials* **2000**, *21*, 31−36.
(18) Ding, B.; Fujimoto, K.; Shiratori, S. Preparation and Characterization of Self-Assembled Polyelectrolyte Multilayered Films on Electrospun Nanofibers. *Thin Solid Films* **2005**, *491*, 23−28.
(19) Nguyen, P. M.; Zacharia, N. S.; Verploegen, E.; Hammond, P. T. Extended Release Antibacterial Layer-by-Layer Films Incorporating Linear-Dendritic Block Copolymer Micelles. *Chem. Mater.* **2007**, *19*, 5524−5530.
(20) Coimbra, P.; Alves, P.; Valente, T.; Santos, R.; Correia, I.; Ferreira, P. Sodium Hyaluronate/Chitosan Polyelectrolyte Complex Scaffolds for Dental Pulp Regeneration: Synthesis and Characterization. *Int. J. Biol. Macromol.* **2011**, *49*, 573−579.
(21) Luppi, B.; Bigucci, F.; Mercolini, L.; Musenga, A.; Sorrenti, M.; Catenacci, L.; Zecchi, V. Novel Mucoadhesive Nasal Inserts Based on Chitosan/Hyaluronate Polyelectrolyte Complexes for Peptide and Protein Delivery. *J. Pharm. Pharmacol.* **2009**, *61*, 151−157.
(22) Mukherjee, S. P.; Davoren, M.; Byrne, H. J. In Vitro Mammalian Cytotoxicological Study of Pamam Dendrimers—Towards Quantitative Structure Activity Relationships. *Toxicol. In Vitro* **2010**, *24*, 169−177.
(23) Sauerbrey, G. The Use of Quartz Oscillators for Weighing Thin Layers and for Microweighing. *Z. Phys.* **1959**, *155*, 206−222.
(24) Liu, G.; Cheng, H.; Yan, L.; Zhang, G. Study of the Kinetics of the Pancake-to-Brush Transition of Poly(*N*-Isopropylacrylamide) Chains. *J. Phys. Chem. B* **2005**, *109*, 22603−22607.
(25) François, P.; Vaudaux, P.; Foster, T. J.; Lew, D. P. Host−Bacteria Interactions in Foreign Body Infections. *Infect. Control* **1996**, *17*, 514−520.
(26) Li, L.; Qian, Y.; Jiang, C.; Lv, Y.; Liu, W.; Zhong, L.; Cai, K.; Li, S.; Yang, L. The Use of Hyaluronan to Regulate Protein Adsorption and Cell Infiltration in Nanofibrous Scaffolds. *Biomaterials* **2012**, *33*, 3428−3445.
(27) Messina, G. M.; Satriano, C.; Marletta, G. A Multitechnique Study of Preferential Protein Adsorption on Hydrophobic and Hydrophilic Plasma-Modified Polymer Surfaces. *Colloids Surf., B* **2009**, *70*, 76−83.
(28) Van Beek, M.; Jones, L.; Sheardown, H. Hyaluronic Acid Containing Hydrogels for the Reduction of Protein Adsorption. *Biomaterials* **2008**, *29*, 780−789.
(29) Hu, X.; Neoh, K.-G.; Shi, Z.; Kang, E.-T.; Poh, C.; Wang, W. An in Vitro Assessment of Titanium Functionalized with Polysaccharides Conjugated with Vascular Endothelial Growth Factor for Enhanced Osseointegration and Inhibition of Bacterial Adhesion. *Biomaterials* **2010**, *31*, 8854−8863.
(30) Zhang, Y.; Zhang, Y.; Chen, M.; Yan, J.; Ye, Z.; Zhou, Y.; Tan, W.; Lang, M. Surface Properties of Amino-Functionalized Poly(E-Caprolactone) Membranes and the Improvement of Human Mesenchymal Stem Cell Behavior. *J. Colloid Interface Sci.* **2012**, *368*, 64−69.
(31) Bourguignon, L. Y. In Hyaluronan-Mediated Cd44 Activation of Rhogtpase Signaling and Cytoskeleton Function Promotes Tumor Progression. *Semin. Cancer Biol.* **2008**, *18*, 251−259.
(32) Takahashi, H.; Takizawa, T.; Matsubara, S.; Ohkuchi, A.; Kuwata, T.; Usui, R.; Matsumoto, H.; Sato, Y.; Fujiwara, H.; Okamoto, A. Extravillous Trophoblast Cell Invasion Is Promoted by the Cd44−Hyaluronic Acid Interaction. *Placenta* **2014**, *35*, 163−170.

DOI: 10.1021/acsami.5b02262
ACS Appl. Mater. Interfaces 2015, 7, 13876−13881